



HAL
open science

Computation of Dispersion Curves in Elastic Waveguides of Arbitrary Cross-section embedded in Infinite Solid Media

Khac-Long Nguyen, Fabien Treyssede, Anne-Sophie Bonnet-Ben Dhia,
Christophe Hazard

► **To cite this version:**

Khac-Long Nguyen, Fabien Treyssede, Anne-Sophie Bonnet-Ben Dhia, Christophe Hazard. Computation of Dispersion Curves in Elastic Waveguides of Arbitrary Cross-section embedded in Infinite Solid Media. 13th International Symposium on Nondestructive Characterization of Materials, May 2013, France. 8p. hal-00948012

HAL Id: hal-00948012

<https://hal.science/hal-00948012>

Submitted on 17 Feb 2014

HAL is a multi-disciplinary open access archive for the deposit and dissemination of scientific research documents, whether they are published or not. The documents may come from teaching and research institutions in France or abroad, or from public or private research centers.

L'archive ouverte pluridisciplinaire **HAL**, est destinée au dépôt et à la diffusion de documents scientifiques de niveau recherche, publiés ou non, émanant des établissements d'enseignement et de recherche français ou étrangers, des laboratoires publics ou privés.

Computation of Dispersion Curves in Elastic Waveguides of Arbitrary Cross-section embedded in Infinite Solid Media

K. Long NGUYEN¹, Fabien TREYSSÈDE¹, A.-S. BONNET-BENDHIA², C. HAZARD²

¹ IFSTTAR, Centre de Nantes, Route de Bouaye; 44344 Bougenais Cedex, France

Phone : +33(0)240845932; e-mail: khac-long.nguyen@ifsttar.fr, fabien.treysede@ifsttar.fr

² ENSTA Paris Tech, 828, Boulevard des Maréchaux; 91762 Palaiseau Cedex, France

Phone : +33(0)181872090; e-mail: anne-sophie.bonnet-bendhia@ensta-paristech.fr, christophe.hazard@ensta-paristech.fr

Abstract

Elastic guided waves are of interest for inspecting structures due to their ability to propagate over long distances. However, guiding structures are often buried in a large domain, considered as unbounded. Waveguides are then open and waves can be trapped or leaky. Analytical tools have been developed to model open solid waveguides but these tools are limited for simple geometries (plates, cylinders). With numerical methods, a difficulty is due to the unbounded geometry. Another issue is due to the presence of leaky modes, which grow exponentially along the transverse directions. The goal of this work is to implement a numerical approach to calculate modes in three dimensional elastic open waveguides, which combines the semi-analytical finite element method and the perfectly matched layers (PML) technique. Both Cartesian and cylindrical PML are implemented.

Keywords: elastic waveguide, leaky mode, semi-analytical finite element, perfectly matched layer.

1. Introduction

For embedded structures, when the velocity of shear waves in the elastic waveguide is greater than in surrounding medium, only leaky modes exist and no trapped modes are present unless the Stoneley waves are allowed by some material combinations [1]. The leakage of energy into the surrounding medium yields attenuation along the guide axis. Such leakage can strongly limit the application of guided wave techniques. An accurate determination of leaky modes appears to be necessary for non destructive evaluation (NDE) of embedded waveguides. Leaky modes have been studied in elastic waveguides to find modes with low attenuation in order to maximize the inspection range [2, 3, 4]. Analytical tools have been developed to model open solid waveguides [5, 6] with simple geometries such as plates and cylinders.

For complex geometries, the modeling often relies on numerical approaches. A rather classical technique is the so-called Semi-Analytical Finite Element (SAFE) method [7, 8], which consists in discretizing the eigenproblem along the transverse directions. Difficulties for the simulation of open waveguides are due to their unbounded section and the exponential growth of leaky modes in the transverse direction. This unusual modal behavior is well-known in electromagnetism [9, 10] and has sometimes been mentioned for elastodynamic waveguides [11, 12]. Analytical studies in electromagnetism have shown that the leaky modes are extraneous solutions of the physical equations but they constitute a good approximation of the excited field over a restricted area, near the core region [21, 22].

A simple numerical procedure has been proposed in [4, 13], which consists in creating artificial viscoelastic layers in order to absorb waves. An alternative approach is the Perfectly Matched Layer (PML) method. This technique has already been applied to the scalar wave equation (i.e. for acoustic, electromagnetic, SH waves) [14, 15]. The combination of SAFE and PML methods has been recently developed to model open solid plate waveguides [16] in two dimensions. The goal of this work is to extend this technique to compute modes in three-

dimensional elastic waveguides buried in a solid matrix. Both Cartesian and cylindrical PML are implemented. It should be mentioned that both kinds of PML have been analyzed from a mathematical point of view for computing the acoustic resonances of open cavities [17, 18].

In Section 2, the variational formulations of SAFE-PML methods are presented for elastic waveguides. In Section 3, numerical solutions are validated thanks to analytical results obtained for a steel bar buried in concrete. The spectra obtained by both types of PML are also compared.

2. Variational formulations

2.1 SAFE - Cartesian PML

2.1.1 Initial formulation

One assumes a linearly elastic material. The time harmonic dependence is chosen as $e^{-i\omega t}$. The section of the open waveguide in the plane (x, y) is supposed to be invariant along the guide axis z . Acoustic sources and external forces are eliminated for the purpose of studying eigenmodes. The variational formulation of the elastodynamic problem is given by :

$$\int_{\tilde{\Omega}} \delta \tilde{\boldsymbol{\epsilon}}^T \tilde{\boldsymbol{\sigma}} d\tilde{\Omega} - \omega^2 \int_{\tilde{\Omega}} \tilde{\rho} \delta \tilde{\mathbf{u}}^T \tilde{\mathbf{u}} d\tilde{\Omega} = 0 \quad (1)$$

where $d\tilde{\Omega} = d\tilde{x}d\tilde{y}d\tilde{z}$ (the tilde notation will be explained in the next subsection).

This formulation holds for any kinematically admissible displacement $\delta \tilde{\mathbf{u}} = [\delta \tilde{u}_x \ \delta \tilde{u}_y \ \delta \tilde{u}_z]^T$. $\delta \tilde{\boldsymbol{\epsilon}} = [\delta \tilde{\epsilon}_{xx} \ \delta \tilde{\epsilon}_{yy} \ \delta \tilde{\epsilon}_{zz} \ 2\delta \tilde{\epsilon}_{xy} \ 2\delta \tilde{\epsilon}_{xz} \ 2\delta \tilde{\epsilon}_{yz}]^T$ denotes the virtual strain vector and $\tilde{\boldsymbol{\sigma}} = [\tilde{\sigma}_{xx} \ \tilde{\sigma}_{yy} \ \tilde{\sigma}_{zz} \ \tilde{\sigma}_{xy} \ \tilde{\sigma}_{xz} \ \tilde{\sigma}_{yz}]^T$ is the stress vector. The superscript T denotes the matrix transpose. $\tilde{\rho}$ is the material density.

The stress-strain relation is $\tilde{\boldsymbol{\sigma}} = \tilde{\mathbf{C}}\tilde{\boldsymbol{\epsilon}}$ where $\tilde{\mathbf{C}}$ is the matrix of material properties. Separating transverse from axial derivatives, the strain-displacement relation can be written as follows :

$$\tilde{\boldsymbol{\epsilon}} = (\mathbf{L}_{\tilde{x}\tilde{y}} + \mathbf{L}_z \partial/\partial \tilde{z}) \tilde{\mathbf{u}} \quad (2)$$

where $\mathbf{L}_{\tilde{x}\tilde{y}}$ is the matrix operator containing derivatives with respect to the \tilde{x}, \tilde{y} directions :

$$\mathbf{L}_{\tilde{x}\tilde{y}} = \begin{bmatrix} \partial/\partial \tilde{x} & 0 & 0 \\ 0 & \partial/\partial \tilde{y} & 0 \\ 0 & 0 & 0 \\ \partial/\partial \tilde{y} & \partial/\partial \tilde{x} & 0 \\ 0 & 0 & \partial/\partial \tilde{x} \\ 0 & 0 & \partial/\partial \tilde{y} \end{bmatrix}, \mathbf{L}_z = \begin{bmatrix} 0 & 0 & 0 \\ 0 & 0 & 0 \\ 0 & 0 & 1 \\ 0 & 0 & 0 \\ 1 & 0 & 0 \\ 0 & 1 & 0 \end{bmatrix} \quad (3)$$

2.1.2 Combining SAFE - Cartesian PML

With PML along the directions x and y , the formulation (1) can be interpreted as the analytical continuation of the equilibrium equations into the complex coordinates \tilde{x}, \tilde{y} with :

$$\tilde{x} = \int_0^x \gamma_x(\xi) d\xi, \quad \tilde{y} = \int_0^y \gamma_y(\xi) d\xi \quad (4)$$

γ_x, γ_y are complex functions of x, y , satisfying :

- $\gamma_x(x) = 1$ for $|x| \leq d_x$; $\gamma_y(y) = 1$ for $|y| \leq d_y$
- $Im\{\gamma_x(x)\} > 0$ for $|x| > d_x$; $Im\{\gamma_y(y)\} > 0$ for $|y| > d_y$

where d_x, d_y are the interface positions between the PML domain and the physical domain (see Fig. 1). In practice, the Cartesian PML is truncated as a rectangle with a boundary condition, arbitrarily chosen (usually of Dirichlet type).

From Eq. (4), the change of variables $\tilde{x} \mapsto x, \tilde{y} \mapsto y$ yields for any function \tilde{f} :

$$\frac{\partial \tilde{f}}{\partial \tilde{x}} = \frac{1}{\gamma_x} \frac{\partial f}{\partial x}, \quad \frac{\partial \tilde{f}}{\partial \tilde{y}} = \frac{1}{\gamma_y} \frac{\partial f}{\partial y}, \quad d\tilde{x} = \gamma_x dx, \quad d\tilde{y} = \gamma_y dy \quad (5)$$

where $\tilde{f}(\tilde{x}(x), \tilde{y}(y), z) = f(x, y, z)$.

In addition to the PML technique, the SAFE method is applied, which consists in assuming an e^{ikz} dependence, where k is the axial wavenumber. Hence, the problem is reduced from three dimensions to two dimensions (from (x, y, z) to the transverse section (x, y)). Combining SAFE and PML methods, the operator matrix $\mathbf{L}_{\tilde{x}\tilde{y}}$ is rewritten by replacing $\partial/\partial\tilde{x}, \partial/\partial\tilde{y}$ by $1/\gamma_x\partial/\partial x, 1/\gamma_y\partial/\partial y$. The strain-displacement relation becomes :

$$\boldsymbol{\epsilon} = (\mathbf{L}_{\tilde{x}\tilde{y}} + ik\mathbf{L}_z)\mathbf{u} \quad (6)$$

Finally, the FE discretization of the variational formulation (1) in the section yields :

$$\{\mathbf{K}_1 - \omega^2\mathbf{M} + ik(\mathbf{K}_2 - \mathbf{K}_2^T) + k^2\mathbf{K}_3\}\mathbf{U} = 0 \quad (7)$$

with the following elementary matrices :

$$\begin{aligned} \mathbf{K}_1^e &= \int_{S^e} \mathbf{N}^{eT} \mathbf{L}_{\tilde{x}\tilde{y}}^T \mathbf{C} \mathbf{L}_{\tilde{x}\tilde{y}} \mathbf{N}^e \gamma_x \gamma_y dx dy, \quad \mathbf{K}_2^e = \int_{S^e} \mathbf{N}^{eT} \mathbf{L}_{\tilde{x}\tilde{y}}^T \mathbf{C} \mathbf{L}_z \mathbf{N}^e \gamma_x \gamma_y dx dy \\ \mathbf{K}_3^e &= \int_{S^e} \mathbf{N}^{eT} \mathbf{L}_z^T \mathbf{C} \mathbf{L}_z \mathbf{N}^e \gamma_x \gamma_y dx dy, \quad \mathbf{K}_4^e = \int_{S^e} \rho \mathbf{N}^{eT} \mathbf{N}^e \gamma_x \gamma_y dx dy \end{aligned} \quad (8)$$

where \mathbf{U} is the global vector of nodal displacements and \mathbf{N}^e is a matrix of nodal interpolating functions on the element e .

Given ω , the eigenproblem (7) is quadratic. The eigensystem can be linearized as [23] :

$$(\mathbf{A} - k\mathbf{B})\hat{\mathbf{U}} = 0 \quad (9)$$

with :

$$\mathbf{A} = \begin{bmatrix} \mathbf{0} & \mathbf{I} \\ \mathbf{K}_1 - \omega^2\mathbf{M} & i(\mathbf{K}_2 - \mathbf{K}_2^T) \end{bmatrix}, \quad \mathbf{B} = \begin{bmatrix} \mathbf{I} & \mathbf{0} \\ \mathbf{0} & -\mathbf{K}_3 \end{bmatrix}, \quad \hat{\mathbf{U}} = \begin{bmatrix} \mathbf{U} \\ k\mathbf{U} \end{bmatrix} \quad (10)$$

Note that, due to the presence of PML layers, $\mathbf{K}_1, \mathbf{K}_3$ and \mathbf{M} are complex matrices and neither \mathbf{A} nor \mathbf{B} are Hermitian.

2.2 SAFE - Cylindrical PML

The formulation (1) can be rewritten in the cylindrical coordinates (r, θ, z) , defined from $(x = r \cos \theta, y = r \sin \theta, z = z)$ as :

$$\int_{\tilde{\Omega}} \delta \tilde{\boldsymbol{\epsilon}}^T \tilde{\boldsymbol{\sigma}} \tilde{r} d\tilde{r} d\theta dz - \omega^2 \int_{\tilde{\Omega}} \tilde{\rho} \delta \tilde{\mathbf{u}}^T \tilde{\mathbf{u}} \tilde{r} d\tilde{r} d\theta dz = 0 \quad (11)$$

where $\tilde{\mathbf{u}} = [\tilde{u}_x(\tilde{r}, \theta, z) \ \tilde{u}_y(\tilde{r}, \theta, z) \ \tilde{u}_z(\tilde{r}, \theta, z)]^T$.

The cylindrical PML defines the complex radial coordinate :

$$\tilde{r} = \int_0^r \gamma(\xi) d\xi \quad (12)$$

where $\gamma(r) = 1$ for $r \leq d$, $Im\{\gamma(r)\} > 0$ for $r > d$ and d is the interface position between the PML and the physical domain (see Fig.1). Note that a cylindrical PML is usually truncated as a circle.

By using the change of variable $\tilde{r} \mapsto r$ and the SAFE method, the strain-displacement relation becomes :

$$\boldsymbol{\epsilon} = (\mathbf{L}_{\tilde{r}\theta} + ik\mathbf{L}_z)\mathbf{u} \quad (13)$$

with :

$$\mathbf{L}_{\tilde{r}\theta} = \begin{bmatrix} \frac{\cos \theta}{\gamma} \frac{\partial}{\partial r} - \frac{\sin \theta}{\tilde{r}} \frac{\partial}{\partial \theta} & 0 & 0 \\ 0 & \frac{\sin \theta}{\gamma} \frac{\partial}{\partial r} + \frac{\cos \theta}{\tilde{r}} \frac{\partial}{\partial \theta} & 0 \\ 0 & 0 & 0 \\ \frac{\sin \theta}{\gamma} \frac{\partial}{\partial r} + \frac{\cos \theta}{\tilde{r}} \frac{\partial}{\partial \theta} & \frac{\cos \theta}{\gamma} \frac{\partial}{\partial r} - \frac{\sin \theta}{\tilde{r}} \frac{\partial}{\partial \theta} & 0 \\ 0 & 0 & \frac{\cos \theta}{\gamma} \frac{\partial}{\partial r} - \frac{\sin \theta}{\tilde{r}} \frac{\partial}{\partial \theta} \\ 0 & 0 & \frac{\sin \theta}{\gamma} \frac{\partial}{\partial r} + \frac{\cos \theta}{\tilde{r}} \frac{\partial}{\partial \theta} \end{bmatrix} \quad (14)$$

Before FE discretization, the formulation (11) and Eq. (13) must be rewritten in Cartesian coordinates. For paper conciseness, the operator matrix $\mathbf{L}_{\tilde{r}\theta}$ in Cartesian coordinates is not presented here.

Finally, it can be shown that the FE discretization of the variation formulation along the transverse section yields the same eigenproblem as Eq. (7), with the elementary matrices :

$$\begin{aligned}
\mathbf{K}_1^e &= \int_{S^e} \mathbf{N}^{eT} \mathbf{L}_{\tilde{r}\theta}^T \mathbf{C} \mathbf{L}_{\tilde{r}\theta} \mathbf{N}^e \frac{\tilde{r}\gamma}{r} dx dy, \mathbf{K}_2^e = \int_{S^e} \mathbf{N}^{eT} \mathbf{L}_{\tilde{r}\theta}^T \mathbf{C} \mathbf{L}_z \mathbf{N}^e \frac{\tilde{r}\gamma}{r} dx dy \\
\mathbf{K}_3^e &= \int_{S^e} \mathbf{N}^{eT} \mathbf{L}_z^T \mathbf{C} \mathbf{L}_z \mathbf{N}^e \frac{\tilde{r}\gamma}{r} dx dy, \mathbf{K}_4^e = \int_{S^e} \rho \mathbf{N}^{eT} \mathbf{N}^e \frac{\tilde{r}\gamma}{r} dx dy
\end{aligned} \tag{15}$$

3. Results

The numerical test considered in this paper is taken from Ref. [4]. It consists of a 10 mm radius steel bar buried in concrete. As the shear velocity in the core is greater than in the surrounding medium, only leaky modes occur.

The longitudinal velocities c_l and shear velocities c_s of materials are respectively : 5960 and 3260 m/s (steel), 4222.1 and 2637.5 m/s (concrete). Densities are : 7.932 g/cm³ (steel) and 2.3 g/cm³ (concrete).

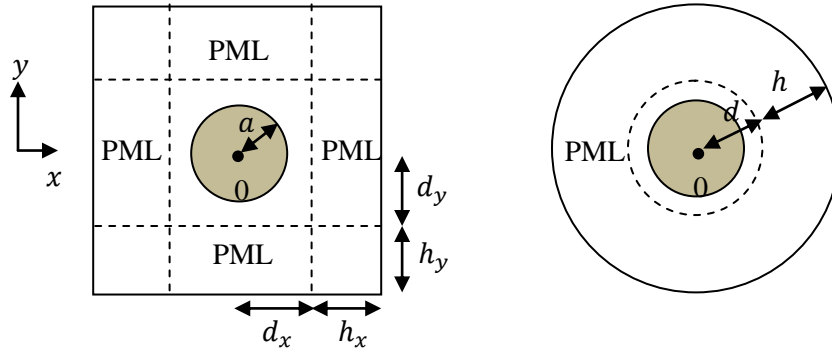


Figure 1. Truncated section of an embedded steel bar in concrete with Cartesian PML (left) and cylindrical PML (right)

The geometry of truncated section for Cartesian and cylindrical PML are represented by Fig. 1. a is the core radius. d_x, d_y, d are the positions of PML interfaces. h_x, h_y, h denote the thickness of PML layers.

The continuity of displacements and stresses is enforced at the steel-concrete interface. Following the suggestion of [14, 17, 20], PML layers are close to the core in order to reduce the effect of exponential growth of leaky modes on the numerical results ($d_x = d_y = d = 1.1a$). A Dirichlet condition is chosen at the exterior boundary of truncated domains. Finite elements are triangles with six nodes. PML functions $\gamma_x, \gamma_y, \gamma$ in Eq. (4) and (12) should be chosen as smooth as possible to minimize numerical reflexion [16]. Their real and imaginary parts are parabolic functions in this work.

3.1 Spectrum of numerical results

Figure 2 represents the spectrum of $\lambda = -k^2$ at the dimensionless frequency $\omega a/c_s = 3.85$, obtained by SAFE-Cartesian and Cylindrical PML methods. Leaky modes are satisfyingly computed with both PML compared to reference values obtained by DISPERSSE [5,6] (circles).

It is observed that PML methods not only provide leaky modes but also non-intrinsic modes corresponding to continua of radiation modes which depend on the characteristics of the PML layer. Such modes resonate mainly in the PML region and they are located along two lines. The effect of PML has been studied in [14, 20] for scalar wave equation. By direct analogy, one can interpret these modes as a discretisation of the continuous spectrum. With elastodynamic, the main difference is that there are two branches corresponding to two continua of shear and longitudinal waves (instead of one with scalar wave problem). The same phenomenon has been observed in the simulation of open elastic plates waveguides with the SAFE-PML method [16]. A modal filtering step can be applied to separate physical modes from radiation modes. The filtering criterion used for our tests is the ratio of kinetic energy in the PML region over the kinetic energy in the whole domain. Physical modes are identified if this criterion is smaller than a user defined value.

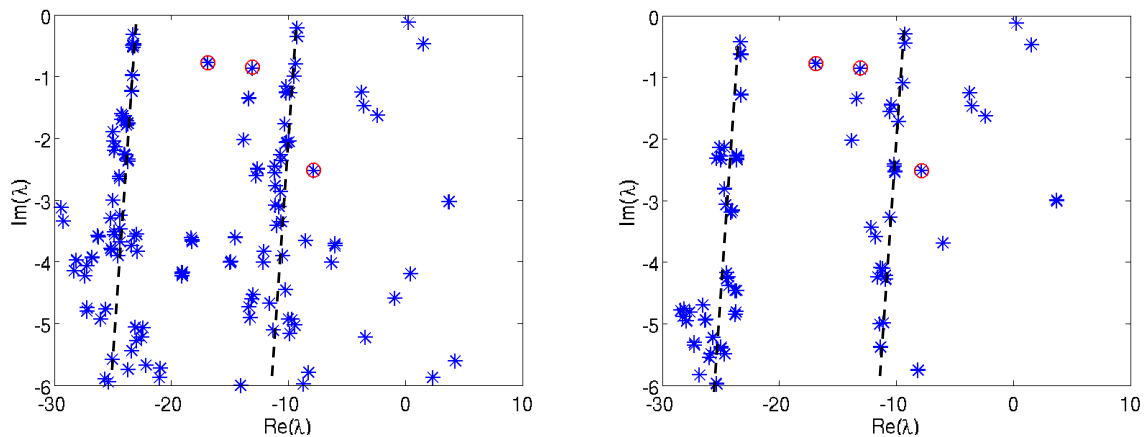


Figure 2. Spectrum of $\lambda = -k^2$ in the complex plane at $\omega a/c_s = 3.85$ (Steel in Concrete) for SAFE-Cartesian PML (left) and SAFE-Cylindrical PML (right). Circles : analytical results, stars : numerical results

In order to compare the computational time, the thickness of Cartesian and cylindrical PML in this subsection has been chosen as $h_x = h_y = 0.9a$ and $h = 1.17a$ in order to approximately have the same number of nodes in the whole domain (about 1700 nodes). According to Fig. 2, more modes must be calculated in the case of Cartesian PML in order to find the first leaky modes. This makes the computation longer for Cartesian PML. The accuracy of each PML is briefly compared in the next subsection.

3.2 Validation

In this section, the dispersion curves obtained after modal filtering are compared to the analytical results of DISPERSE. The thickness of PML in Cartesian and radial directions is the same ($h_x = h_y = h = 0.9a$).

Figure 3 represents the phase velocity V_p/c_s and the attenuation $Im(ka)$ along the axis as a function of the dimensionless frequencies $\omega a/c_s$ computed with the SAFE-Cartesian PML, the SAFE-Cylindrical PML and DISPERSE. Analytical curves correspond to the L(0,1) mode (longitudinal mode) and the F(1,1) and F(1,2) modes (flexural modes). The other modes whose analytical results have not been calculated correspond to modes with higher order (F(1,3), F(2,1),...).

Good agreement between the numerical and analytical results can be observed for both PML techniques. In term of the computational cost, the thickness of cylindrical PML domain has been reduced to $0.9a$ (instead of $1.17a$ in Sec. 3.1). The computational time of cylindrical PML now becomes significantly lower than the Cartesian PML (5 times lower).

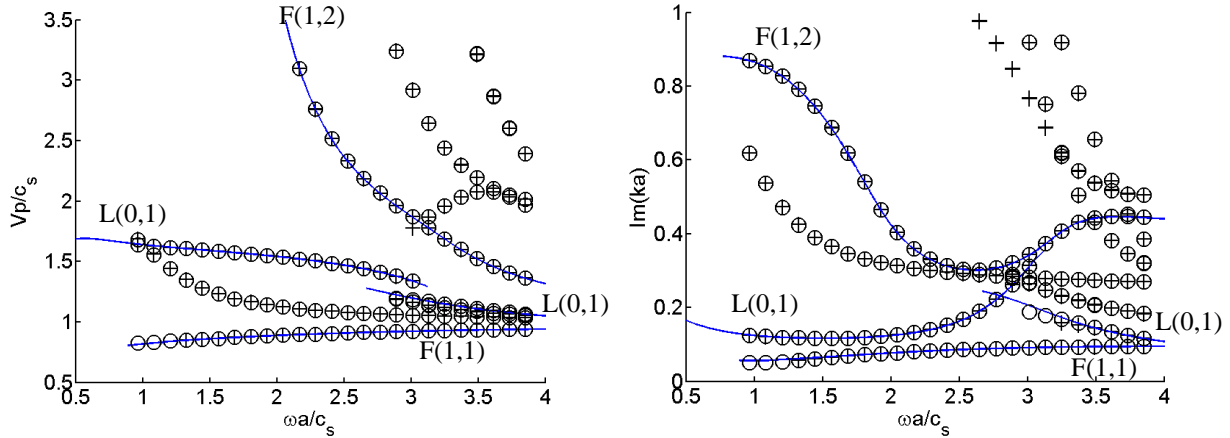


Figure 3. Comparison of SAFE-PML methods with analytical results. Circles : results with Cartesian method, crosses : results with cylindrical PML, continuous curves : analytical results for four modes

4. Conclusion

The combination of SAFE and two PML methods has been implemented and validated through a test case of simple geometry with known analytical solutions : a cylindrical solid bar embedded in a solid medium. From a computational point of view, the cylindrical PML seems to be better than Cartesian PML.

The present work is motivated by the non-destructive testing cables, usually constituted by multi-wire helical strand embedded in a solid matrix. In order to extend the SAFE method proposed for helical structures in [19] to open cross-section, PML along twisting directions will be developed.

References

1. R. N. Thurston, ‘Elastic-waves in rods and clad rods, Journal of the Acoustical Society of America’, 64(1):1–37, 1978.
2. M. J. S. Lowe and P. Cawley, ‘Comparison of the modal properties of a stiff layer embedded in a solid medium with the minima of the plane-wave reflection coefficient’, Journal of the Acoustical Society of America, 97(3):1625–1637, 1995.
3. N. Ryden and M. J. S. Lowe, ‘Guided wave propagation in three-layer pavement structures’, Journal of the Acoustical Society of America, 116(5):2902–2913, 2004.
4. Michel Castaings and Michael Lowe, ‘Finite element model for waves guided along solid systems of arbitrary section coupled to infinite solid media’, Journal of the Acoustical Society of America, 123(2):696–708, 2008.
5. M. J. S. Lowe, ‘Plate waves for the NDT of diffusion bonded titanium’, PhD thesis, Mechanical Engineering Department, Imperial College London, 1992.
6. B. Pavlakovic, ‘Leaky guided ultrasonic waves in NDT’, PhD thesis, Mechanical Engineering Department, Imperial College London, 1998.

7. T. Hayashi, W.-J. Song, and J. L. Rose, 'Guided wave dispersion curves for a bar with an arbitrary cross-section, a rod and rail example', *Ultrasonics*, 41:175–183, 2003.
8. I. Bartoli, A. Marzani, F. Lanza di Scalea, and E. Viola, 'Modeling wave propagation in damped waveguides of arbitrary cross-section', *Journal of Sound and Vibration*, 295:685–707, 2006.
9. R. E. Collin, 'Field Theory of Guided Waves', IEEE Press, 1991.
10. J. Hu and C. R. Menyuk, 'Understanding leaky modes: slab waveguide revisited', *Advances in Optics and Photonics*, 1:58–106, 2009.
11. J. A. Simmons, E. Drescherkrasicka, and H. N. G. Wadley, 'Leaky axisymmetrical modes in infinite clad rods', *Journal of the Acoustical Society of America*, 92(2):1061–1090, 1992.
12. A. C. Hladky-Hennion, P. Langlet, and M. de Billy, 'Conical radiating waves from immersed wedges', *Journal of the Acoustical Society of America*, 108(6):3079–3083, 2000.
13. Z. Fan, M. J. S. Lowe, M. Castaings, and C. Bacon, 'Torsional waves propagation along a waveguide of arbitrary cross section immersed in a perfect fluid', *Journal of the Acoustical Society of America*, 124(4):2002–2010, 2008.
14. A. S. Bonnet-BenDiha, B. Goursaud, C. Hazard and A. Prieto, 'Finite element computation of leaky modes in stratified waveguides', In 5th Meeting of the Anglo-French-Research-Group, Vol 128, pp73-86, 2008.
15. A. S. Bonnet-BenDiha, B. Goursaud, C. Hazard and A. Prieto, 'A multimodal method for non-uniform open waveguides', *International Congress on Ultrasonics, Proceedings*, 3(1):497-503, 2010.
16. F. Treyssède, K. L. Nguyen, A.-S. Bonnet-BenDhia and C. Hazard, 'On the use of a SAFE-PML technique for modeling two-dimensional open elastic waveguides', *Acoustics 2012*, Nantes (France), 667-672, April 23-27, 2012.
17. S. Kim and J.-E. Pasciak, 'The computation of resonances in open systems using a perfectly matched layer', *American Mathematical Society*, Vol 78, No 267, pp 1375-1398, 2009.
18. S. Kim and J.-E. Pasciak, 'Analysis of a Cartesian PML approximation to acoustic scattering problems in \mathbb{R}^2 ', *J. Math. Anal. Appl.*, 370:168-186, 2010.
19. F. Treyssède, 'Elastic waves in helical waveguides', *Wave Motion*, 45:457-470, 2008.
20. B. Goursaud, 'Étude mathématique et numérique de guides d'ondes ouverts non uniformes, par approche modale(Mathematical and numerical study of non uniform open waveguides, modal approach, in French', PhD thesis, École Polytechnique, 2010.
21. J. Hu and C. R. Menyuk, 'Understanding leaky modes : slab waveguide revisited', *Advanced in Optics and Photonics*, 1:58-106, 2009.
22. R. E. Collin, 'Field theory of guided waves', CaseWestern reserve university, 1991.
23. Vahan Baronian, 'Couplage des methods modale et éléments finis pour la diffraction des ondes élastiques guideés', PhD Thesis, École Doctorale de l'École Plytechnique, 2009.